NASA Technical Memorandum 81165

Turbulence Measurements in the Boundary Layer of a Low-Speed Wind Tunnel Using Laser Velocimetry

Edward T. Schairer

February 1980

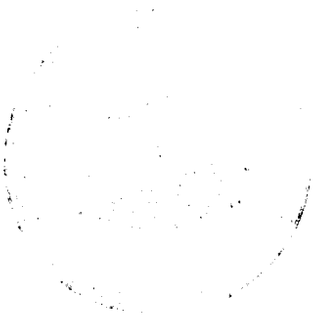

National Aeronautics and
Space Administration

NASA Technical Memorandum 81165

Turbulence Measurements in the Boundary Layer of a Low-Speed Wind Tunnel Using Laser Velocimetry

Edward T. Schairer, Ames Research Center, Moffett Field, California

NASA
National Aeronautics and
Space Administration

Ames Research Center
Moffett Field, California 94035

TURBULENCE MEASUREMENTS IN THE BOUNDARY LAYER OF A LOW-SPEED WIND TUNNEL USING LASER VELOCIMETRY

Edward T. Schairer

Ames Research Center

SUMMARY

This report describes laser velocimeter measurements in an incompressible, turbulent boundary layer along the wall of a low-speed wind tunnel. The laser data are compared with existing hot-wire anemometer measurements of a flat plate, incompressible, turbulent, boundary layer with zero pressure gradient. An argument is presented to explain why previous laser velocimeter measurements in zero pressure gradient, turbulent boundary layers have shown an unexpected decrease in turbulent shear stresses near the wall.

INTRODUCTION

Laser velocimeter measurements in zero pressure gradient, supersonic boundary layers have consistently shown an unexpected decrease in the turbulent shear stresses in the inner portion of the boundary layer (refs. 1-3). Whether this decrease is an actual feature of these flows or is due to inherent errors in the measurement technique has been debated in the literature (refs. 4 and 5). Because of the difficulty of obtaining hot-wire measurements in compressible flows, there are few hot-wire anemometer shear stress data at supersonic conditions to compare with the laser data. There are, however, reliable hot-wire measurements of incompressible, turbulent boundary layers (ref. 6). Therefore, a comparison of laser velocimeter measurements of shear stresses in an incompressible, turbulent boundary layer with existing hot-wire data should provide information about the accuracy of laser velocimeter shear stress measurements. Anomalies in the incompressible boundary-layer data might help explain the supersonic data.

This report describes laser velocimeter measurements in an incompressible, turbulent boundary layer along the wall of a low-speed wind tunnel. Special attention was given to obtaining shear stress measurements as close to the wall as possible. The laser data are compared with hot-wire anemometer measurements of a flat plate, incompressible, turbulent boundary layer with no streamwise pressure gradient (ref. 6).

The experiment was conducted in the Ames 25- by 35-cm Subsonic Wind Tunnel. A flat plate at zero incidence was approximated by the top wall of

the constant area rectangular test section. Conditions in the test section were a stagnation temperature of nominally room temperature, Mach number of 0.20, and a unit Reynolds number of 4×10^5 per meter. Velocity data were acquired at a single streamwise station where the boundary-layer thickness was about 1.5 cm (0.59 in.). A single-component, dual scatter laser velocimeter was used in forward scatter.

EXPERIMENT

The Ames 25- by 35-cm Wind Tunnel (fig. 1) is an indraft, nonreturn wind tunnel. Vacuum is supplied by the same compressors which evacuate and pressurize the transonic wind tunnels of the unitary plan wind-tunnel facilities. The tunnel Mach number is set by adjusting the area of a choked nozzle downstream of the test section.

The test section is illustrated in figure 2. The length/height ratio of the constant area section is 2.6:1. The boundary-layer measurement location was on the centerline of the top wall about 34 boundary-layer thicknesses downstream of the beginning of the constant area section. Static pressures were measured along the centerline of the top wall at 7.62 cm (3.0 in.) intervals with water manometers. The static pressure gradient across the boundary layer was assumed to be zero. Three-dimensional effects were assumed to be negligible because the boundary layer was thin compared to the test section width (a ratio of 16:1).

A pitot probe that could traverse normal to the wall (across the boundary layer) was located at the boundary-layer measurement station on the centerline of the upper wall. The position of the probe was measured with a dial indicator to an accuracy of 0.051 mm (0.002 in.). The dynamic pressure in the boundary layer was measured by connecting the pitot probe to one side and the wall static orifice nearest the measurement station to the other side of a precision water manometer. These measurements were accurate to within about 0.75 N/m^2 (0.015 psf). Velocities were computed from the dynamic pressures accounting for differences in temperature and atmospheric pressure from one run to the next.

The laser velocimeter is illustrated schematically in figure 3. It is a single-velocity component, fringe-mode system operated in forward scatter. The laser was a 4-W argon-ion laser operating at a wavelength of 5145 Å.

The interference fringe spacing (Δs) was about 21.5 μm. A Bragg cell produced a 40-MHz frequency difference (Δf_{Bragg}) between the interfering beams, causing the fringes to move normal to themselves at the rate

$$V_{fringe} = \Delta s \, \Delta f_{Bragg}$$

$$= 21.5 \ \mu m \times 40 \ MHz = 860 \ m/s$$

The fringe motion eliminated directional ambiguity and provided sensitivity to particles with small flow angles relative to the fringe orientation.

The transmitting lens and two mirrors were mounted on a positioning platform, allowing the laser measurement point to be changed by moving only the lens and mirrors while the laser and the rest of the transmitting optics remained fixed. The diameter of the volume of intersection of the two laser beams, which determined the spatial resolution of the velocimeter, was estimated to be about 300 μm (0.012 in.). This estimate was based on photographs of a single particle burst on the display of an oscilloscope.

Light scattered by particles passing through the measurement volume was collected by a simple lens and focussed on the pinhole of a photodetector. The lens and photodetector were mounted on a positioning platform on the opposite side of the test section as the transmitting optics.

The output of the photodetector was a high-frequency voltage oscillation of frequency given by

$$f_{signal} = \frac{V_\perp}{\Delta s} + \Delta f_{Bragg}$$

where $V_\perp$ is the particle's velocity perpendicular to the fringe orientation. The signal frequency was reduced to a value closer to the velocity-induced frequency ("Doppler frequency" = $V_\perp/\Delta s$) by mixing it (Hewlett-Packard passive diode mixer) with the output of a sine-wave generator (f_{mix}):

$$f_{signal} = \frac{V_\perp}{\Delta s} + \Delta f_{Bragg} - f_{mix}$$

For typical streamwise velocity measurements (U = 63 m/s), the Doppler frequency was 2.8 MHz, the Bragg cell frequency was 40 MHz, and the sine-wave generator frequency was 32 MHz, yielding a signal frequency of 10.8 MHz.

A Macrodyne LDV signal processor was used to measure the period of the mixed signal by counting the number of cycles of a 500-MHz clock which elapsed in the course of eight cycles of the input signal. This number was output in binary form to a Northern Tracor pulse height analyzer which constructed a histogram of signal periods as the data were acquired. A Hewlett-Packard 9830 calculator was programmed to convert the pulse height analyzer histogram into a particle velocity distribution.

Signals from about 1000 particles were used to produce a velocity distribution at each location. Naturally occurring dust particles, many of which probably were substantially larger than 1 μm, were the light scattering sources. Within about 0.7 mm (0.030 in.) of the wind-tunnel wall the signal/noise ratio deteriorated because light scattered from the wall itself resulted in significantly lower data rates. Thus laser measurements within 0.7 mm of the wall were sometimes based on as few as 100 particles. Measurements near the wall were repeated at least once. No laser data could be obtained closer than 0.25 mm (0.0098 in.) from the wall.

The mean and standard deviation were computed for every velocity distribution:

$$\overline{V}_\perp = \frac{1}{N} \sum_i V_{\perp_i} \qquad \text{(Mean)}$$

$$\langle \overline{V}_\perp \rangle = \sqrt{\overline{V_\perp^2}_i - \overline{V}_\perp^2} \qquad \text{(Standard deviation)}$$

where N is the total number of measurements.

The position of the laser beams in the test section was set manually by using the tip of the pitot probe as a target. The maximum position error of the laser measurement point was about 0.4 mm (0.016 in.) or 2.6% of the boundary-layer thickness. This is greater than the probe position uncertainty because of the finite dimensions of the probe tip and the laser beam measurement volume.

RESULTS

The streamwise static pressures along the centerline of the top wall of the test section are illustrated in figure 4. As expected for a constant area duct, there was a slightly favorable streamwise pressure gradient (about -174 N/m^2 per m) due to the displacement effect of the boundary layer. In addition, the contraction at the upstream end of the test section produced an adverse pressure gradient (about 3266 N/m^2 per m) at the beginning of the constant area section. This was about 22 boundary-layer thicknesses upstream of the measurement station. Thus the wind-tunnel wall only approximated a flat plate at zero incidence.

The mean streamwise velocity in the boundary layer was independently computed at each point from the dynamic pressure data and the laser velocimeter data. The resulting velocity profiles are compared in figure 5. The pressure data were based on between 4 and 15 independent measurements at each location and were typically repeatable to within 2.5%. The laser data points were based on between 1 and 3 measurements at each station (each measurement based on about 1000 particles) and were repeatable to within 1%. The pressure data have not been adjusted for displacement effects, nor have the laser data been corrected for velocity biasing (ref. 7).

In the free stream, the laser velocity measurements were about 1.8% lower than the pitot tube measurements. This difference is about the same as the uncertainty of the interference fringe spacing measurement and thus was not unexpected. The laser data were corrected for this error by forcing the laser data to agree with the pressure data at one point in the free stream.

The corrected laser mean velocity measurements were consistently lower than the pressure measurements in the inner portion of the boundary layer

(fig. 5). In a study by Dimotakis (ref. 5), good agreement was obtained between velocity profiles measured with a laser velocimeter and with a pitot probe for M = 0.11. However, for M > 0.8 the velocities measured with the laser velocimeter were consistently lower than those obtained with a pitot probe, similar to the present results. Dimotakis also found that, for M = 0.11, a correction for velocity biasing (ref. 7) produced a negligible change in the laser mean velocity data.

A possible explanation for the low laser mean velocity measurements near the wall was the decrease in signal/noise ratio due to "flare." As the noise increased close to the wall, only relatively large particles scattered enough light to produce measurable signals. If the smallest particles that produced a measurable signal became too large, they would not accurately follow the flow. Since naturally occurring room dust served as scattering sources, there is little doubt that large particles (10 × 1 μm) were present.

Normal velocities were measured directly by aligning the interference fringes parallel to the streamwise axis of the tunnel. The measured mean normal velocity distribution across the boundary layer fell within a band ±1% of the free-stream streamwise velocity. This measurement uncertainty was larger than the maximum expected normal velocity for a flat-plate boundary layer. A net flow toward the wall as reported by Dimotakis (ref. 5) was not evident.

For a flow in which mean velocities are independent of time, streamwise and normal turbulent fluctuations are given by

$$u_i' = u_i - \overline{u}$$

and

$$v_i' = v_i - \overline{v}$$

respectively, where u_i and v_i are instantaneous velocities and $\overline{u}$ and $\overline{v}$ are time averages. The streamwise and normal turbulence intensities $\langle u' \rangle$ and $\langle v' \rangle$ are defined as the root mean square (RMS) or standard deviations of the turbulent fluctuations as given by

$$\langle u' \rangle = \sqrt{\overline{u'^2}} = \sqrt{\overline{u_i^2} - \overline{u}^2}$$

$$\langle v' \rangle = \sqrt{\overline{v'^2}} = \sqrt{\overline{v_i^2} - \overline{v}^2}$$

Both velocity fluctuations and measurement uncertainty due to noise contributed to the measured deviations from the mean. If the noise and velocity (Doppler) signals are assumed to be statistically independent and to have Gaussian distributions, then the variance (standard deviation squared) of the signal frequency is given by

$$\sigma^2_{f_{signal}} = \sigma^2_{f_{Doppler}} + \sigma^2_{f_{noise}}$$

where $\sigma_{f_{Doppler}}$ and $\sigma_{f_{noise}}$ are the standard deviations of the signal frequency due to velocity variations and noise, respectively. If the RMS noise level ($\sigma_{f_{noise}}$) relative to the mean signal frequency ($\overline{f}_{signal}$) were known, then the turbulence intensity could be corrected for noise by

$$\langle v' \rangle = \sigma_{f_{Doppler}} \times \Delta s$$

$$= \overline{f}_{signal} \sqrt{\left(\frac{\sigma_{f_{signal}}}{\overline{f}_{signal}}\right)^2 - \left(\frac{\sigma_{f_{noise}}}{\overline{f}_{signal}}\right)^2} \times \Delta s \qquad (1)$$

The free-stream turbulence intensity of the 25- by 35-cm wind tunnel was previously measured with a hot-wire anemometer and found to be 0.083% of the free-stream velocity (58 m/s) (ref. 8). Turbulence levels as low as this are beyond the resolution of the present laser velocimeter because the signal broadening due to noise was at least as great as the turbulence. Uncorrected measurements in the free stream with the laser velocimeter consistently produced streamwise turbulence intensities $\langle u' \rangle / U_\infty$ of about 3% where U_∞ is the free-stream velocity. By assuming a minimum RMS noise level relative to the mean signal frequency of 0.5% ($\sigma_{f_{noise}} / \overline{f}_{signal} = 0.005$), and "correcting" the turbulence intensity for this noise according to equation (1), the free-stream streamwise turbulence intensity became zero. Uncorrected normal free-stream turbulence intensities $\langle v' \rangle / U_\infty$ measured with the laser were only slightly higher than 3% but, when corrected for 0.5% signal noise, they were still about 1.5%.

Figure 6 illustrates the turbulence intensities in the boundary layer in the streamwise direction $\langle u' \rangle$ and normal to the wall $\langle v' \rangle$. All the data were corrected for a minimum RMS noise level relative to the signal frequency of 0.5% according to equation (1). This correction, however, becomes negligible as the velocity fluctuation levels become large. The turbulence levels are shown normalized with respect to the free-stream velocity U_∞ as well as the wall skin-friction velocity u_τ = (shear stress at the wall/density)$^{1/2}$.

Also illustrated in figure 6 are the hot-wire measurements of Klebanoff (ref. 6). Fortuitously, the skin-friction coefficient from reference 6 and the skin-friction coefficient measured in this experiment were nearly identical ($c_f = 0.00275$). Thus there was no shift of the data reported here relative to Klebanoff's between turbulence intensities normalized with respect to U_∞ and u_τ.

It is not clear why the apparent normal turbulence intensity $\langle v' \rangle$ was greater than the streamwise turbulence near the edge of the boundary layer.

The noise correction affected the streamwise turbulence measurements more than the normal turbulence measurements because the mean signal frequency was higher for the streamwise measurements than for the normal measurements, whereas the standard deviations of the signals were about equal (see eq. (1)).

The turbulent shear stress at each point in the boundary layer was determined by independently measuring velocity components oriented ±45° to the free-stream direction and forming half the difference of the respective velocity distribution variances:

$$\frac{\tau}{\rho} = -\overline{u'v'} = \frac{(\sigma_{+45}^2 - \sigma_{-45}^2)}{2} \tag{2a}$$

$$\sigma_{+45}^2 = \frac{\overline{u'^2}}{2} + \overline{u'v'} + \frac{\overline{v'^2}}{2} \tag{2b}$$

$$\sigma_{-45}^2 = \frac{\overline{u'^2}}{2} - \overline{u'v'} + \frac{\overline{v'^2}}{2} \tag{2c}$$

Since the velocity variances were independently measured several times at each station, a matrix of shear stresses was produced using equation (2a) and all combinations of ±45° measurements. This matrix served as a statistical sample from which the mean shear stress and standard deviation of the shear stress measurements were computed at each point. The resulting shear stresses, normalized with respect to the shear stress at the wall, are illustrated in figure 7. The shear stress coefficient at the wall ($c_{f_{wall}} = 0.00275$) was estimated from a law-of-the-wall fit of the mean streamwise velocity profile (ref. 9).

Noise should not bias shear stress measurements as it does turbulence intensities if the noise and turbulence levels are statistically independent and if the mean squared noise for ±45° velocity component measurements are equal at a given boundary-layer station. Therefore, no noise correction was applied to the shear stress measurements.

The uncertainty in the shear stress measurements increased at locations close to the wall both because of the increase in noise due to flare and the increase in turbulence intensities close to the wall (fig. 6). The variances of the ±45° velocity distributions included contributions due to streamwise and normal turbulence intensities as well as noise (eqs. (2b) and (2c)). As these contributions increased relative to the cross-correlation $\overline{u'v'}$, the uncertainty in the shear stress contribution increased (fig. 7).

Figure 7 also includes Klebanoff's hot-wire measurements of an incompressible, turbulent, flat-plate boundary layer with zero streamwise pressure gradient ($\partial p/\partial x = 0$)(ref. 6). The shear stress (τ) approaches the wall shear stress with zero slope ($\partial\tau/\partial y = 0$), consistent with the relationship

$$\frac{\partial \tau}{\partial y} = \frac{\partial p}{\partial x} = 0$$

which follows from the momentum equation near the wall where the convection terms are negligible. The dashed line in figure 7 represents the expected slope of the shear stress distribution at the wall for the present experiment in which the streamwise pressure gradient was $-174\ N/m^2$ per m. The scatter in the shear stress data precludes defining $\partial\tau/\partial y$ at the wall; however it is significant that the measured shear stresses do not decrease near the wall.

The correlation coefficient $\overline{u'v'}/\langle u' \rangle \langle v' \rangle$ is a measure of the correlation between u and v velocity fluctuations. With a single-component velocimeter, its value at any point is found from at least four independent measurements: two to find $\overline{u'v'}$ and one each to find $\langle u' \rangle$ and $\langle v' \rangle$. In reality, all of these quantities were measured several times at each measurement location. Thus, the correlation coefficient at each point was computed from all possible combinations of $\langle u' \rangle$, $\langle v' \rangle$, and $\overline{u'v'}$ measurements at that point; $\langle u' \rangle$ and $\langle v' \rangle$ were adjusted for a minimum noise RMS of 0.5% of the signal frequency. The mean value and the standard deviation of the resulting distribution of values of the correlation coefficient at each measurement station are illustrated in figure 8. Also shown for comparison are Klebanoff's results (ref. 6).

Outside the boundary layer the correlation coefficient is very small because the turbulent shear stress is near zero. Within the boundary layer, as the wall is approached, the shear stress increases as do the velocity fluctuations $\langle u' \rangle$ and $\langle v' \rangle$. According to Klebanoff, the correlation coefficient reaches a constant level of about -0.49. The presence of noise should reduce the level of the correlation coefficient from its actual level since noise increases $\langle u' \rangle$ and $\langle v' \rangle$ (denominator) but, in the ideal case, does not bias shear stress measurements (numerator). Figure 8 shows that near the wall the correlation coefficient increased slightly, an indication that the shear stress measurements near the wall are high.

DISCUSSION

Unlike the findings of Johnson and Rose (ref. 1), Yanta and Lee (ref. 2), Abbis (ref. 3), and Dimotakis et al. (ref. 5), the turbulent shear stress measurements illustrated in figure 7 do not decrease close to the wall. However, the scatter of the shear stress measurements near the wall is roughly 20% of the mean shear stress at the wall and makes conclusions based on these data highly speculative.

Dimotakis (ref. 5) measured a consistent falloff in shear stresses near the wall even in an incompressible boundary layer. This is particularly disturbing because it is in conflict with the hot-wire measurements of Klebanoff (ref. 6) and thus suggests a laser velocimeter measurement error. Dimotakis' conclusion was that near the wall there is a net flow of particles toward the wall which produces low laser velocimeter measurements of shear stress.

One important difference between the present experiment and the work of those reporting a dropoff in turbulent shear stresses near the wall was the use of a Bragg cell in this experiment. Data acquired using stationary fringes (no Bragg cell) are biased against particles whose directions make small angles relative to the fringe direction because, beyond some angle, these particles will not cross the required eight fringes needed to produce a processable signal. Fringe motion perpendicular to the fringe direction eliminates this bias.

The following heuristic argument, suggested by D. A. Johnson of Ames Research Center (private communication, 1979), is offered to explain how stationary fringes might produce shear stress measurements lower than the actual shear stress. Consider a point in a turbulent boundary layer at which the mean flow velocity is parallel to the wall and where there are turbulent fluctuations u' and v' (fig. 9). The velocity distribution variances measured by fringes oriented ±45° to the streamwise direction are given by equations (2b) and (2c). If turbulent fluctuations u' and v' are large enough, particles with the combination of -u' and -v' will be underrepresented by measurements with fringes oriented at +45° because the flow angles of these particles are more nearly parallel to the fringes than for other combinations of u' and v' (fig. 9). Thus measurements with +45° fringe orientation will be biased against positive values for u'v'. Similarly, velocity measurements with -45° fringe orientation will be biased against negative values for u'v' since particles with the combination of -u' and +v' will be underrepresented.

If $\overline{u'v'} = 0$, then the probability of a particle having -u' and -v' equals the probability of a particle having -u' and +v'. Thus the bias of the +45° fringe measurement would be exactly offset by the bias of the -45° fringe measurement, and an accurate value for $\overline{u'v'}$ would result.

In an incompressible, zero-pressure-gradient, turbulent boundary layer we know $\overline{u'v'} < 0$ since $\overline{u'v'}/\langle u'\rangle\langle v'\rangle < 0$ (fig. 8) and $\langle u'\rangle$ and $\langle v'\rangle$ must be greater than zero. Therefore, the probability of a particle having the combination of -u' and +v' ($u'v' < 0$) is greater than for the combination of -u' and -v' ($u'v' > 0$). Thus, the bias of the -45° measurement toward less negative values of u'v' is not completely offset by the opposite bias of the +45° measurement. The result is a value for $\overline{u'v'}$ which is less negative than the true value. Since $\tau/\rho = -\overline{u'v'}$, this means that if u' and v' are large enough, the measured shear stress using stationary ±45° fringe orientations will be lower than the actual shear stress.

This biasing would only be expected when the turbulent fluctuations became large enough relative to the mean local flow velocity to produce significant instantaneous flow angles. This is most likely to occur very close to the wall where turbulence levels are highest. Figure 6 shows that in the present experiment at $y/\delta = 0.02$:

$$\langle u' \rangle = 0.10 \times U_\infty$$

$$= 0.10 \times 63 \text{ m/s} = 6.3 \text{ m/s}$$

$$\langle v' \rangle = 0.04 \times U_\infty$$

$$= 0.04 \times 63 \text{ m/s} = 2.5 \text{ m/s}$$

The local mean velocity at $y/\delta = 0.02$ was (fig. 5):

$$u_{local} = 0.55 \times U_\infty$$

$$= 0.55 \times 63 \text{ m/s} = 34.6 \text{ m/s}$$

Thus the instantaneous flow angle relative to the streamwise direction corresponding to $-\langle u' \rangle$ and $+\langle v' \rangle$ was

$$\alpha = \tan^{-1}\left(\frac{\langle v' \rangle}{\overline{u}_{local} - \langle u' \rangle}\right)$$

$$= \tan^{-1}\left(\frac{2.5}{34.6 - 6.3}\right)$$

$$= 5.1°$$

The limiting flow angle that could occur can be estimated by taking u' to be -3.0 standard deviations from $\overline{u'}(=0)$ and v' to be +3.0 standard deviations from $\overline{v'}(=0)$:

$$\alpha_{limit} = \tan^{-1}\left(\frac{3\langle v' \rangle}{\overline{u}_{local} - 3\langle u' \rangle}\right)$$

$$= \tan^{-1}\left(\frac{3(2.5)}{34.6 - 3(6.3)}\right)$$

$$= 25.7° \text{ relative to streamwise direction}$$

$$= 19.3° \text{ relative to } -45° \text{ fringe direction}$$

A crude estimate of the critical angle relative to the fringe direction below which there would be insufficient fringe crossings to produce a usable signal is given by

$$\beta_{critical} = \tan^{-1}\frac{n\Delta s}{d}$$

$$= \tan^{-1}\frac{n}{N}$$

where n is the required number of fringe crossings (8 crossings), Δs is the fringe spacing (21.5 μm), d is the diameter of the measurement volume (300 μm), and $N = d/\Delta s$ is the number of fringes in the measurement volume (13.9). In the present experiment, this angle was

$$\beta_{critical} = \tan^{-1}\left(\frac{8 \times 21.5\ \mu m}{300\ \mu m}\right)$$

$$= \tan^{-1}\left(\frac{8}{13.9}\right)$$

$$= 29.8°$$

Above we found that it was probable that some particles had flow angles as small as 19.3° relative to the fringes; thus, had the fringes been stationary, it is likely the data would have been biased.

The question of low shear stress measurements near a wall could best be resolved by making measurements with a two-velocity component laser velocimeter. Such a system has been successfully used to measure the boundary layer of an airfoil in transonic flows (ref. 10). The advantage of a two-component velocimeter is that it measures the u and v components of each particle simultaneously. The turbulent shear stress can then be computed from the statistical sample:

$$\frac{\tau}{\rho} = -\overline{u'v'} = -(\overline{uv} - \bar{u}\,\bar{v})$$

Simultaneous measurement of u and v ensures that both measurements are made at the same point in the boundary layer and that the test section conditions are identical for both measurements; it also improves the probability that signal noise will not bias the shear stress measurement. Conversely, measurements made with no correlation in time, as is required with a single-component velocimeter, are subject to position error, changes in tunnel conditions, and changes in signal noise between one measurement and the next.

The disadvantages of a two-component laser velocimeter are the increased expense and the complication. In addition, positioning a matrix of four converging laser beams at a point near a surface might compromise the ideal incidence angle of each pair of beams positioned independently resulting in increased noise due to flare.

SUMMARY

An experiment was conducted to measure turbulent fluctuations and shear stresses in the boundary layer of a low-speed wind tunnel using a one-component laser velocimeter. Measurements in the portion of the boundary layer closest to the free stream were made without difficulty and compared well with the results of other investigators. Measurements very near the wall were hampered

by signal noise and were typified by low data rates and high scatter of the data. The measurements, however, gave no indication of a dropoff in shear stress near the wall.

Unlike the measurements of those reporting a dropoff in shear stress near the wall, the measurements reported here were made with a laser velocimeter that produced moving interference fringes. An argument is presented suggesting that, if $\overline{u'v'}$ is negative and turbulence intensities are high enough, measurements of shear stress near the wall made with stationary fringes will be lower than the actual shear stress.

REFERENCES

1. Johnson, D. A.; and Rose, W. C.: Laser Velocimeter and Hot-Wire Anemometer Comparison in a Supersonic Boundary Layer. AIAA J., vol. 13, no. 4, April 1975.

2. Yanta, W. J.; and Lee, R. E.: Measurements of Mach 3 Turbulence Transport Properties on a Nozzle Wall. AIAA J., vol. 14, no. 6, 1976.

3. Abbis, J. B.: Development of Photon Correlation Anemometry for Application to Supersonic Flow. AGARD CP-193, Applications of Non-Intrusive Instrumentation in Fluid Flow Research, 1976, pp. 11.1-11.11.

4. Sandborn, V. A.: A Review of Turbulence Measurements in Compressible Flow. NASA TM X-62,337, 1974.

5. Dimotakis, P. E.; Collins, D. J.; and Lang, D. B.: Laser Doppler Velocity Measurements in Subsonic, Transonic, and Supersonic Turbulent Boundary Layers. Preprint, presented at the Third International Workshop on Laser Velocimetry, Purdue University, July 11-13, 1978.

6. Klebanoff, P. S.: Characteristics of Turbulence in a Boundary Layer with Zero Pressure Gradient. NACA TR 1247, 1955.

7. McLaughin, D. K.; and Tederman, W. G.: Biasing Correction for Individual Realization of Laser Anemometer Measurements in Turbulent Flows. Phys. Fluids, vol. 16, no. 12, Dec. 1973.

8. Davis, Sanford S.: Measurements of Discrete Vortex Noise in a Closed-Throat Wind Tunnel. In Aeroacoustics; STOL Noise; Airframe and Airfoil Noise, Ira R. Schwartz, ed., AIAA, 1976.

9. Allen, J. M.; and Tudor, D. H.: Charts for Interpolation of Local Skin Friction from Experimental Turbulent Velocity Profiles. NASA SP-3048, 1969.

10. Johnson, D. A.; and Bachalo, W. D.: Transonic Flow About a Two-Dimensional Airfoil - Inviscid and Turbulent Flow Properties. AIAA Paper 78-1117, 1978.

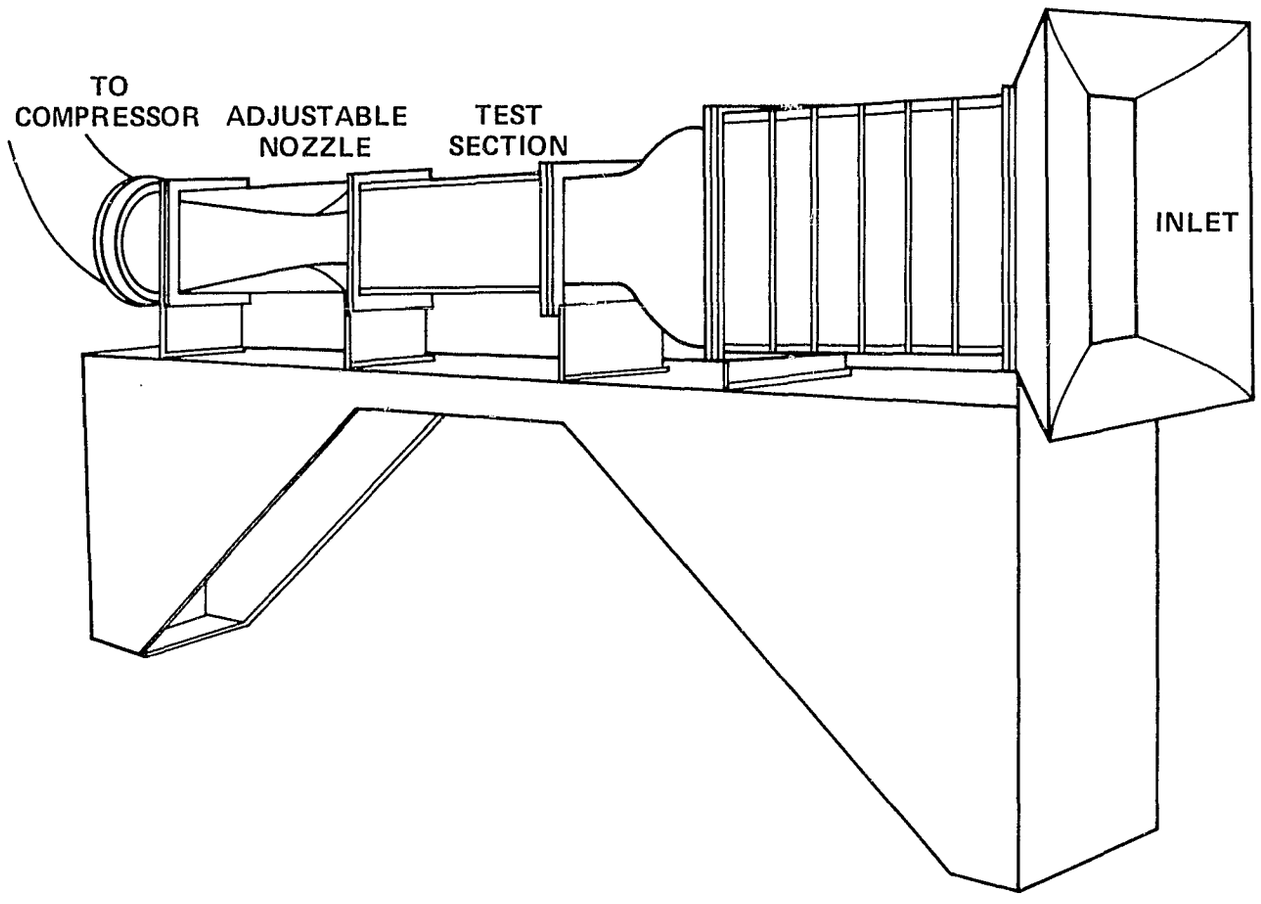

Figure 1. Ames 25- by 35-cm Wind Tunnel.

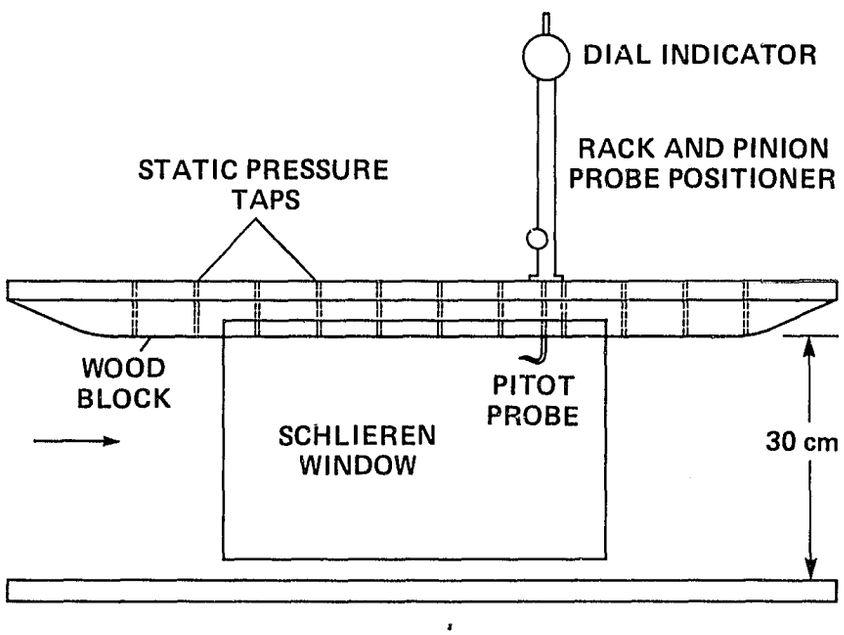

Figure 2. Test section.

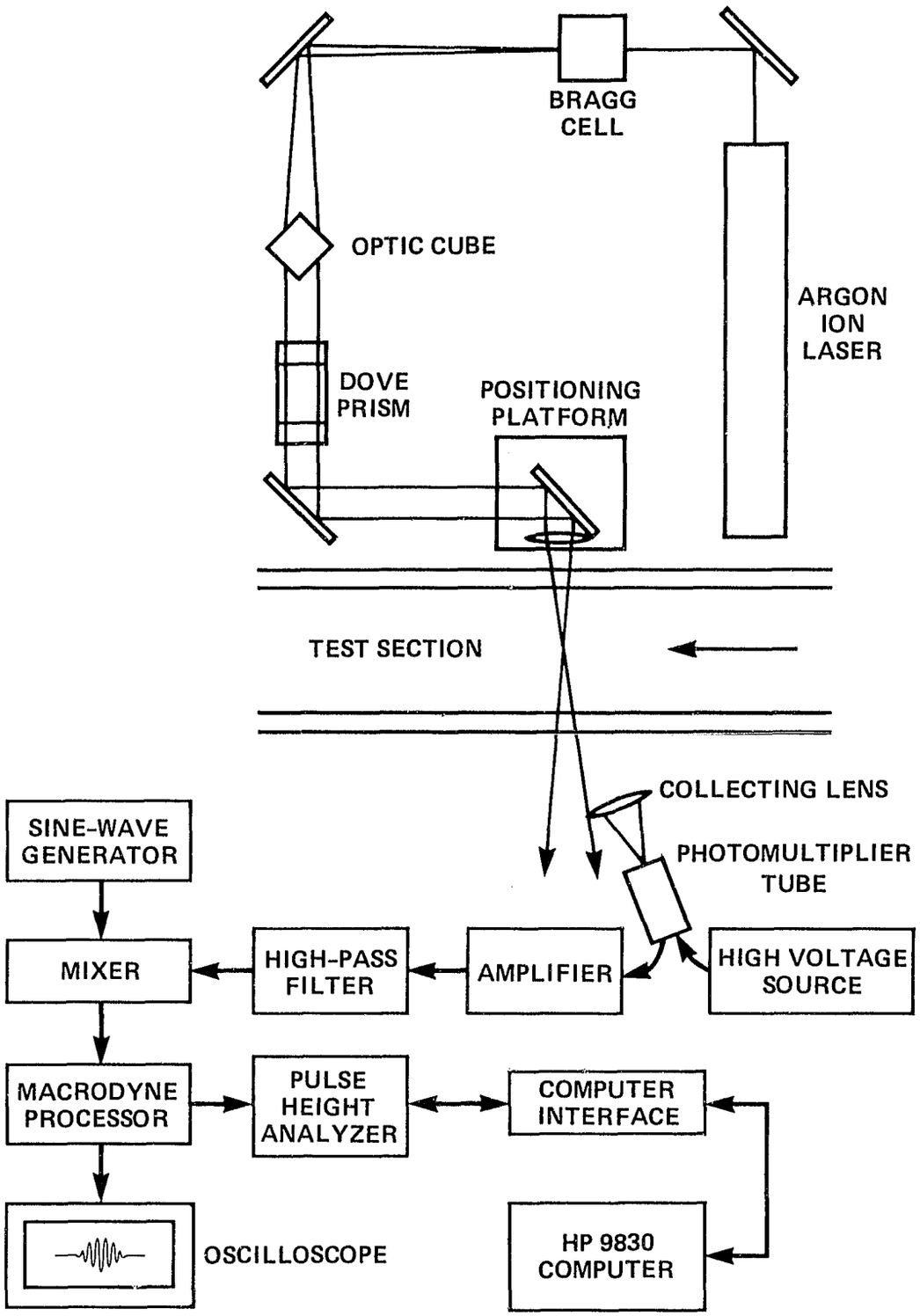

Figure 3. Laser velocimeter.

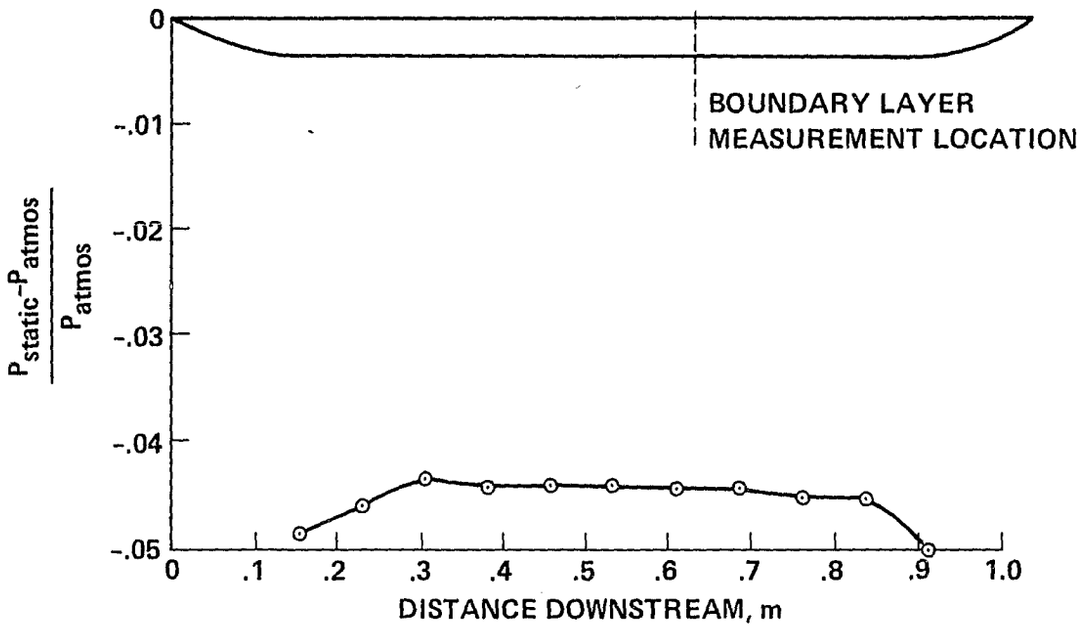

Figure 4. Streamwise static pressure.

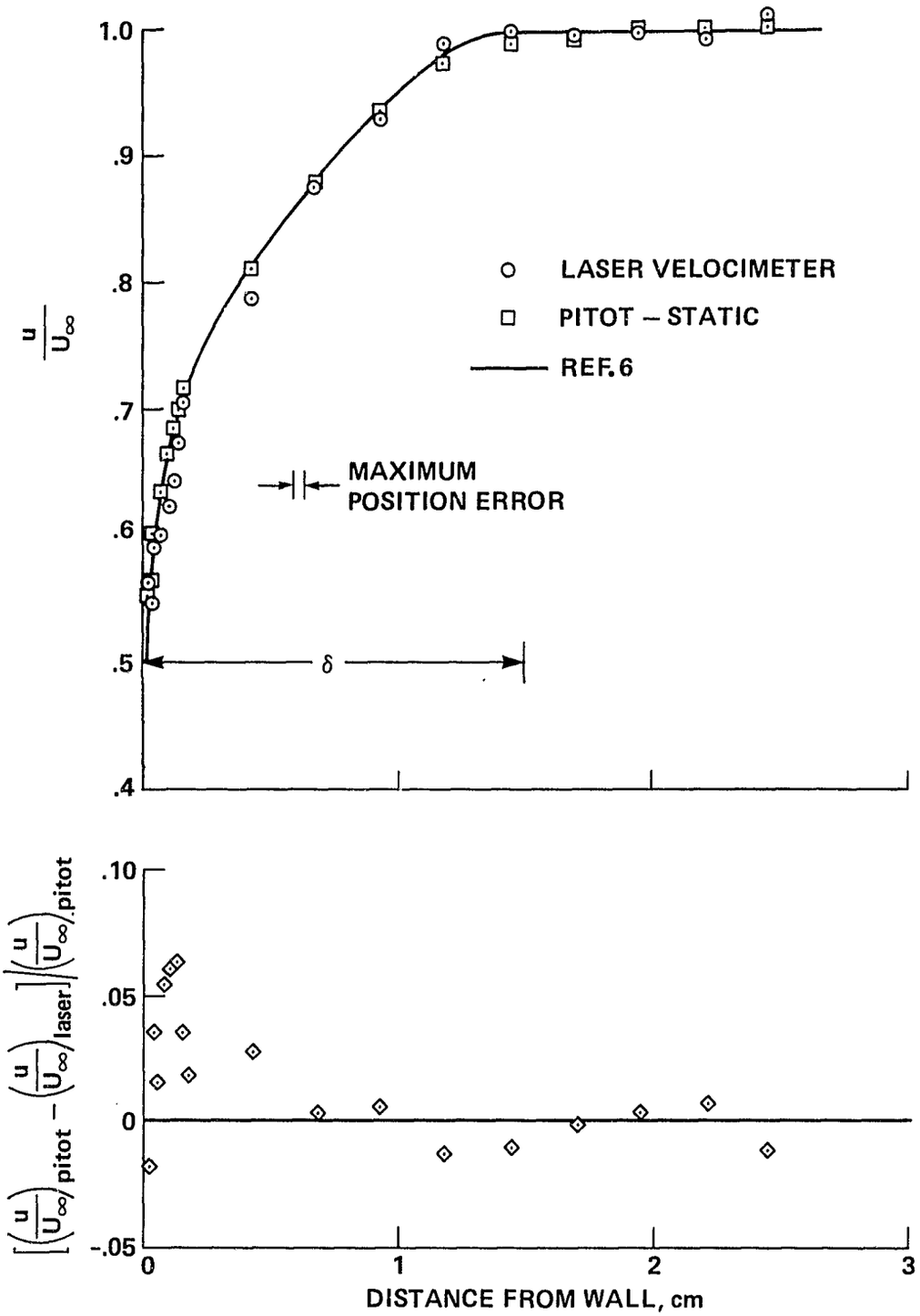

Figure 5. Normalized velocity profile.

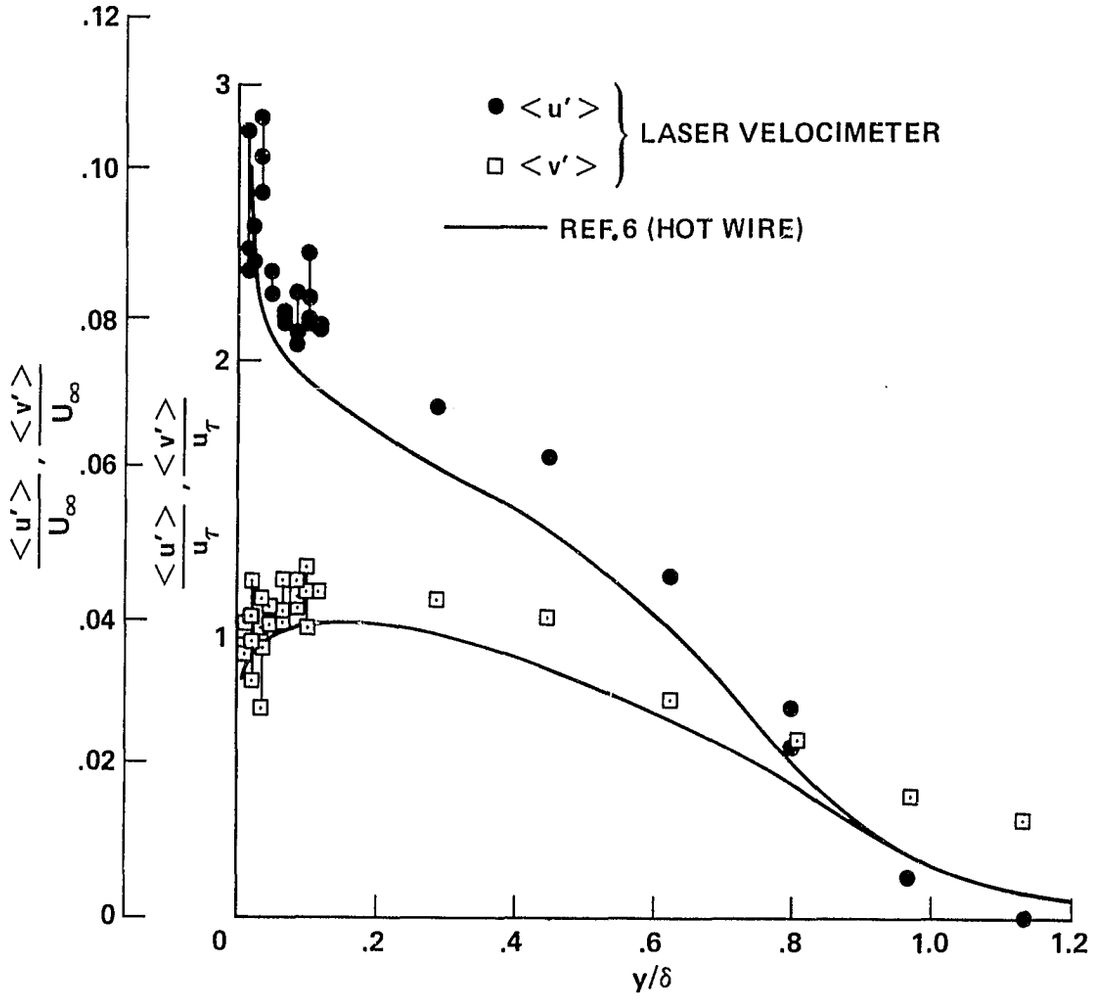

Figure 6. Turbulence intensities.

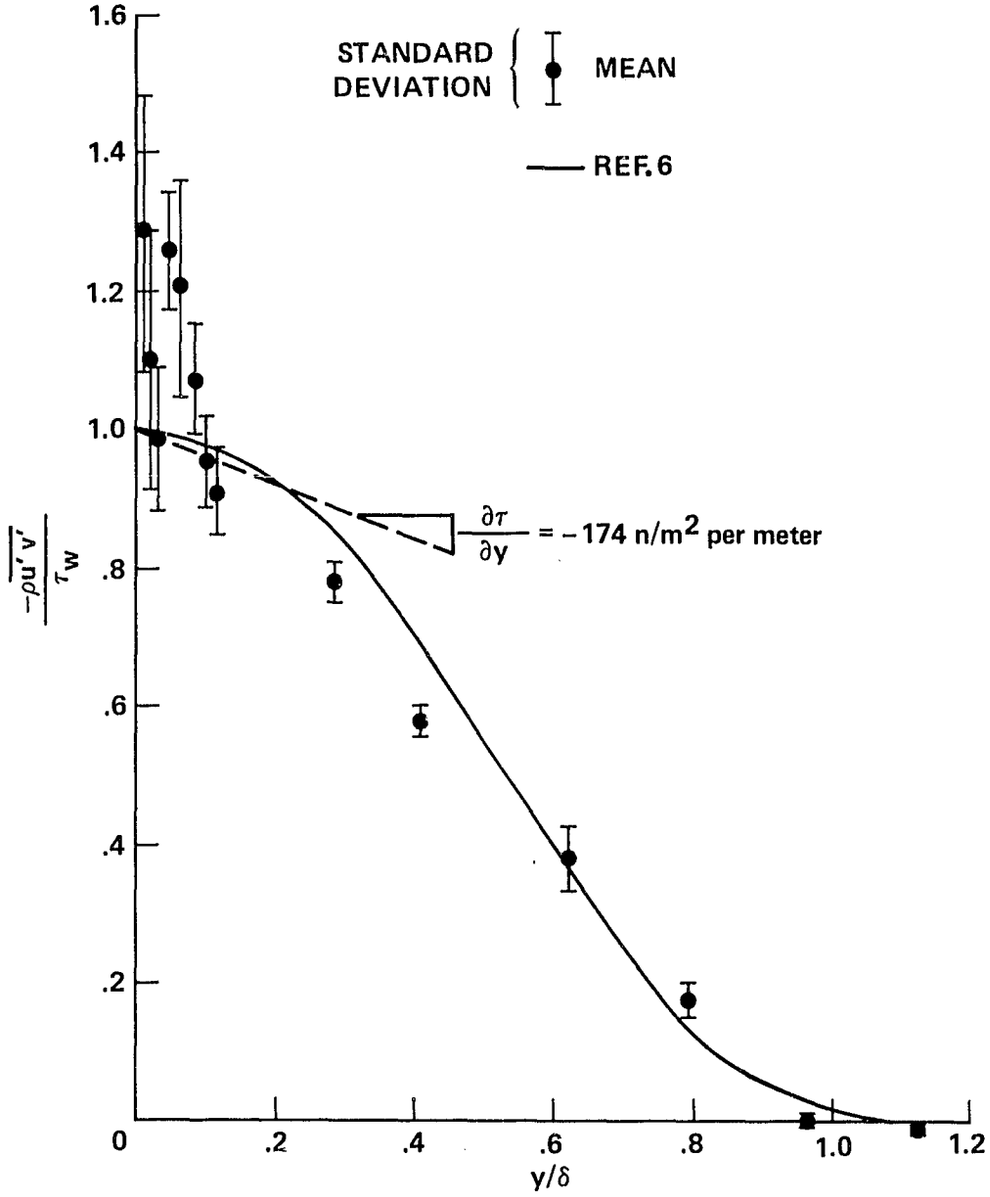

Figure 7. Turbulent shear stresses.

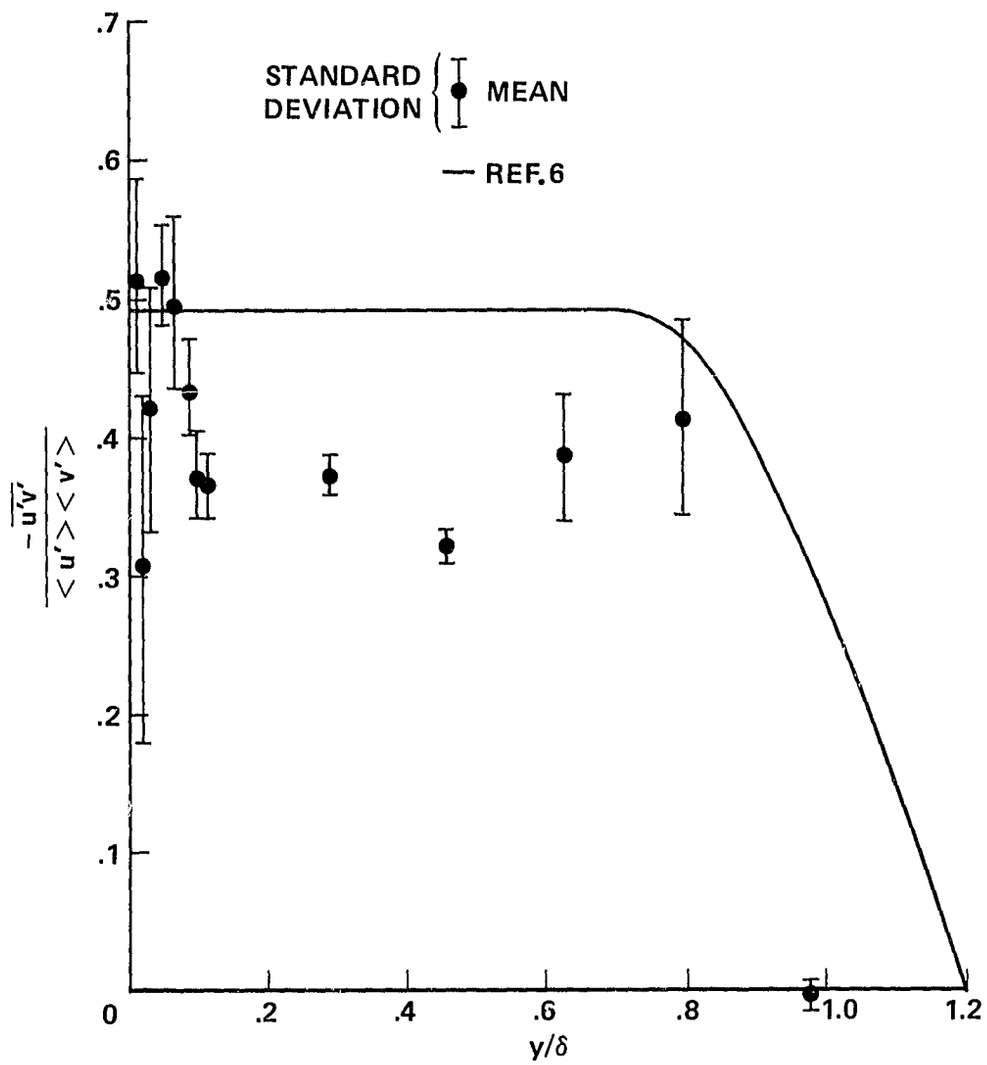

Figure 8. Correlation coefficient.

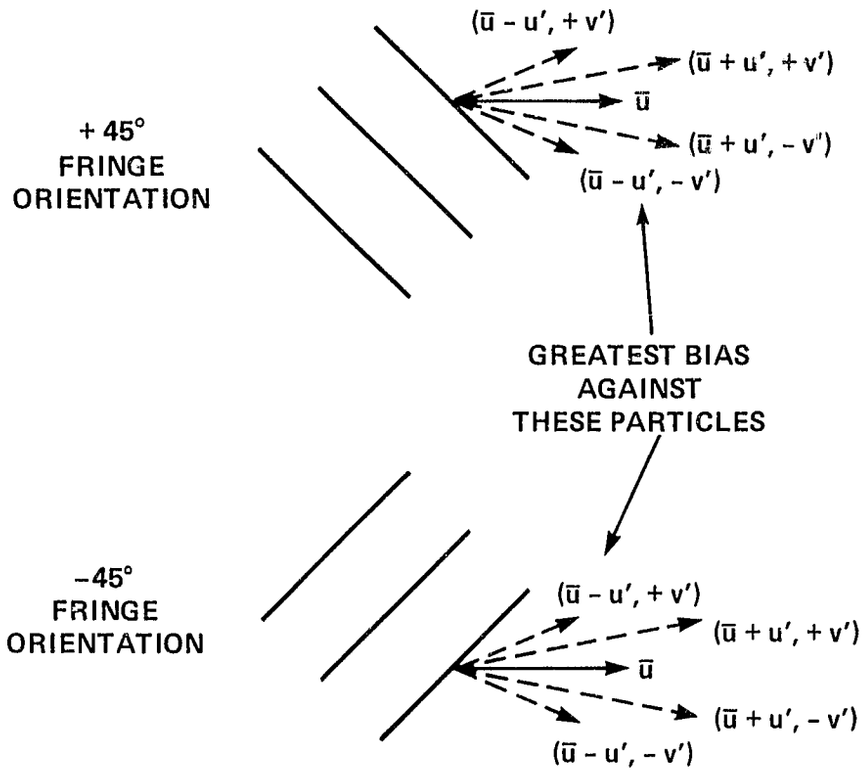

Figure 9. Fringe geometry shear stress measurements.

1. Report No.	2. Government Accession No.	3. Recipient's Catalog No.
NASA TM-81165		

4. Title and Subtitle	5. Report Date
TURBULENCE MEASUREMENTS IN THE BOUNDARY LAYER OF A LOW-SPEED WIND TUNNEL USING LASER VELOCIMETRY	6. Performing Organization Code

7. Author(s)	8. Performing Organization Report No.
Edward T. Schairer	A-8058
	10. Work Unit No. 505-31-21
9. Performing Organization Name and Address	11. Contract or Grant No.
NASA Ames Research Center Moffett Field, Calif. 94035	
	13. Type of Report and Period Covered
12. Sponsoring Agency Name and Address	Technical Memorandum
National Aeronautics and Space Administration Washington, D. C. 20546	14. Sponsoring Agency Code

15. Supplementary Notes

16. Abstract

This report describes laser velocimeter measurements in an incompressible, turbulent boundary layer along the wall of a low-speed wind tunnel. The laser data are compared with existing hot-wire anemometer measurements of a flat plate, incompressible, turbulent, boundary layer with zero pressure gradient. An argument is presented to explain why previous laser velocimeter measurements in zero pressure gradient, turbulent boundary layers have shown an unexpected decrease in turbulent shear stresses near the wall.

17. Key Words (Suggested by Author(s))	18. Distribution Statement
Aerodynamics Fluid mechanics and heat transfer Lasers and masers	Unlimited STAR Category - 34

19. Security Classif. (of this report)	20. Security Classif. (of this page)	21. No. of Pages	22. Price*
Unclassified	Unclassified	24	$4.00

*For sale by the National Technical Information Service, Springfield, Virginia 22161